Glassy behavior in martensites: Interplay between elastic anisotropy and disorder in zero-field-cooling/field-cooling simulation experiments

Pol Lloveras,[1,2] Teresa Castán,[1,2] Marcel Porta,[1,2,3] Antoni Planes,[1,2] and Avadh Saxena[2,3]
[1]*Departament d'Estructura i Constituents de la Matèria, Universitat de Barcelona, Diagonal 647, 08028 Barcelona, Catalonia, Spain*
[2]*Institut de Nanociència i Nanotecnologia, Universitat de Barcelona, Diagonal 647, 08028 Barcelona, Spain*
[3]*Theoretical Division, Los Alamos National Laboratory, Los Alamos, New Mexico 87545, USA*
(Received 26 May 2009; published 17 August 2009)

We study the combined effect of elastic anisotropy and disorder on the microstructure and thermodynamic behavior in alloys undergoing a martensitic transformation. Within a Ginzburg-Landau free-energy framework we find the region in the parameter space where a ferroelastic glassy state exists without twinning. We find that such a glassy state is of kinetic origin rather than due to geometrical frustration. The glassy behavior is characterized by simulating zero-field-cooling/field-cooling curves for different values of anisotropy and disorder. Finally, we discuss experimental implications for Fe-Pd and Ni-Ti alloys.

DOI: 10.1103/PhysRevB.80.054107 PACS number(s): 64.70.K−, 81.30.Kf, 62.20.D−

I. INTRODUCTION

Materials termed as martensites[1] include a large number of metals and alloys with the common feature of undergoing a structural transition that is known to be diffusionless. As a consequence, the product phase is characterized by the presence of differently oriented variants (commonly twin related) of equal energy and structure depending on the specific crystal symmetry of the parent phase. Associated with this ferroelastic character, a subclass of such materials with displacive transitions also exhibits superelasticity and shape memory effect. However, the martensitic *family* is wide and comprises very different materials each one with specific peculiarities. Let us focus, for instance, on Fe-Pd and Ni-Ti (cubic) alloy systems. Fe-Pd undergoes a weakly first-order fcc-to-fct (face centered tetragonal) transition[2] and shows pretransitional phenomena known as "tweed."[3] This refers to the strongly anisotropic pattern observed by transmission electron microscopy and identified as diagonal striations of small strain.[4] Concerning Ni-Ti, it undergoes a strongly first-order B2-to-B19′ transition[5] and exhibits very rich pretransitional behavior but no signature of tweed contrast has been observed. Actually,[6] when conveniently doped, dark-field electron-diffraction experiments have revealed that the morphology of the precursor structure is mottledlike, corresponding to very small distorted regions of almost spherical shape. It has been suggested[6,7] that these differences in the behavior of the two materials in the precursor regime arise from the anisotropy of the elastic constants, defined as $\mathcal{A}=C_{44}/C'$, that turns out to be about six to seven times[8] larger in Fe-Pd ($\mathcal{A}\sim 12-15$) (Ref. 2) than in Ni-Ti ($\mathcal{A}\sim 2$) (Ref. 5).

Another general and important feature in martensites is the strong dependence of the transition temperature on the alloy composition. For instance, Fe_xPd_{1-x} undergoes for $x=0.71$ a martensitic transition (MT) at room temperature but for $x=0.68$ the transition temperature drops to 0 K.[9] Similarly, in Ni_xTi_{1-x} the martensitic transition is suppressed when composition is varied from stoichiometry $x=0.5$ to 0.515. It is worth mentioning that for $x\geq 0.51$, Ni-Ti exhibits some characteristic glassy behavior.[10,11]

A standard experiment for detecting signatures of glassy behavior is the so-called zero-(stress)-field-cooling (ZFC)/field-cooling (FC) measurements.[12] The method consists of comparing the two strain curves obtained by applying a small stress upon heating, following a cooling under zero stress (ZFC) in one case and under nonzero (but low enough[13]) stress (FC) in the other. Deviations between the two curves are indicative of history dependence, generally associated with glassy behavior, as typically observed in spin glasses,[14] relaxor ferroelectrics,[15] and recently also in $Ni_{51.5}Ti_{48.5}$ ferroelastic strain glass.[11] Beyond the fundamental differences among such disparate systems, they all have in common the presence of some sort of disorder (giving rise to multiple metastable states) inside a conventional, nonglassy ferroic system.[11]

Previous studies[16,17] have shown that Ginzburg-Landau theory including long-range anisotropic interactions is appropriate to model the MT due to, among other reasons, its athermal character. Also, it succeeds in obtaining pretransitional tweed textures due to either thermal fluctuations or the presence of static disorder. Within the latter framework, in a recent paper[7] we focused on the influence of elastic anisotropy on the structural patterns and associated thermodynamic responses in martensites, obtaining good qualitative agreement with experiments. Particularly, we found glassy behavior in ZFC simulation experiments for low values of both temperature (T) and anisotropy ($\mathcal{A}$). We now extend the previous study to include the effect of disorder intensity (σ) and its interplay with $\mathcal{A}$. Variations in disorder should be understood as arising from composition changes, doping or quenching effects. Concerning the elastic anisotropy $\mathcal{A}$, significant variations necessarily entail changing the material.

Our results show that glassy behavior can be obtained for any value of $\mathcal{A}$, provided σ is higher than a critical value, σ^*, which in turn depends on $\mathcal{A}$ and $\sigma^*(\mathcal{A})$, in such a way that the higher the value of $\mathcal{A}$ the higher is the required σ^*. The structural patterns observed for a wide range of parameters have been characterized in real and reciprocal spaces. In particular, we have studied the thermodynamic free-energy behavior and the domain size distribution. Moreover, we have systematically computed the ZFC/FC strain curves for differ-

ent values of σ and $\mathcal{A}$. From these we have been able to identify the existence of a crossover behavior between twinned and glassy martensites in terms of model parameters σ and $\mathcal{A}$. We emphasize that no geometrical frustration has been found to be associated with such glassy states. Rather, our results suggest that glassy behavior in martensites is of kinetic origin due to the existence of local energy barriers arising from disorder. This is in agreement with previous experiments in Ni-Ti alloys.[10,11]

The paper is organized as follows: in Sec. II we summarize the model and discuss the aspects relevant for the present work. The numerical results are presented in Sec. III. Last section is devoted to the discussion and experimental implications.

II. MODEL

We use a Ginzburg-Landau generic model for square-to-rectangular MT. It represents a two-dimensional (2D) counterpart of a real three-dimensional case corresponding, for instance, to the cubic-to-tetragonal MT in Fe-Pd. The three homogeneous modes available in a square lattice—symmetry adapted strains—are the so-called bulk, deviatoric, and shear strains, defined as $e_1=\frac{1}{\sqrt{2}}(\epsilon_{xx}+\epsilon_{yy})$, $e_2=\frac{1}{\sqrt{2}}(\epsilon_{xx}-\epsilon_{yy})$, and $e_3=\epsilon_{xy}$, respectively, where ϵ_{ij} refer to the linear strain tensor components. In our case the order parameter (OP) is the deviatoric strain e_2 since it stands for rectangular deformations. The Ginzburg-Landau free-energy density can be then written as

$$f_{GL}(e_2)=\frac{A_2(T)}{2}e_2^2-\frac{\beta}{4}e_2^4+\frac{\gamma}{6}e_2^6+\frac{\kappa}{2}|\nabla e_2|^2, \tag{1}$$

where A_2 is a function of T and β, γ, and κ are phenomenological coefficients. The resulting triple well potential accounts for the first-order character of the transition, with a low-temperature phase with two minima corresponding to the two possible rectangular orientations of the unit cell, i.e., the two variants giving rise to twinning. In addition, the remaining e_1 and e_3 strains are also taken into account up to the harmonic level: $f_{\text{nonOP}}(e_1,e_3)=\frac{A_1}{2}e_1^2+\frac{A_3}{2}e_3^2$. However, the St. Vénant compatibility condition links e_1, e_2, and e_3 since in 2D there exist only two degrees of freedom corresponding to the underlying displacement field $\vec{u}=(u_x,u_y)$. Moreover, since the variable is e_2 only, e_1 and e_3 must take the values that minimize the total free energy. Hence, compatibility constraints and energy minimization yield a nonlocal $f_{\text{nonOP}}(e_2)$ in real space (with a $1/r^2$ falloff[18] in 2D) which gives rise to collective and cooperative cell motions that are at the origin, for instance, of tweed textures and martensitic twins. The total free-energy density will be then the sum of two contributions,

$$f(\vec{r})=f_{GL}(\vec{r})+\int f_{\text{nonOP}}(\vec{r},\vec{r}')d\vec{r}', \tag{2}$$

where we have specified the dependence of each term on the position vector in real space ($\vec{r}$) through the strain field $e_2(\vec{r})$.

The long-range potential f_{nonOP} can be expressed locally in Fourier space,

$$f_{\text{nonOP}}(\vec{k})=\frac{A_3}{2}\frac{(k_x^2-k_y^2)^2}{(A_3/A_1)k^4+8(k_xk_y)^2}|e_2(\vec{k})|^2. \tag{3}$$

The $(k_x^2-k_y^2)^2$ factor intrinsically entails the directionality of f_{nonOP} that leads to the diagonal interfaces observed in both patterns. Note that in terms of model parameters, the elastic anisotropy[19] is $\mathcal{A}=A_3/2A_2$ so that, at $T\approx$ const, $\mathcal{A}\sim A_3$. As mentioned in the introduction, inhomogeneities are a necessary ingredient for tweed precursors, often observed in these materials. Also, they are at the origin of the observed glassy behavior, which we shall focus on in this work. The fundamental role played by such spatial inhomogeneities arising from intrinsic statistical compositional variations, off-stoichiometry, lattice imperfections, etc., is taken into account here by means of a quenched-in spatially fluctuating field included in the harmonic coefficient $A_2(T)$ so that now $A_2(T,\vec{r})=\alpha_T[T-T_c-\eta(\vec{r})]$, where T_c is the low stability limit of the high-temperature phase in the clean limit (no disorder). Here, $\eta(\vec{r})$ is the disorder variable, spatially correlated by means of an exponential pair-correlation function $G(r)$ and Gaussian distributed with zero mean. Mathematically, this is expressed by

$$G(r)=\langle\eta(\vec{r}')\eta(\vec{r}'-\vec{r})\rangle\propto e^{-r/\xi},$$

$$g(\eta)=\frac{1}{\sqrt{2\pi}\sigma}e^{-\eta^2/2\sigma^2}, \tag{4}$$

where ξ is the correlation length and σ the standard deviation (i.e., the amplitude) of the Gaussian distribution and determines the intensity of disorder. Note that the disorder produces a distribution of characteristic temperatures, in particular, of stability limits $\tilde{T}_c(\vec{r})\equiv T_c+\eta(\vec{r})$ and transition temperatures $\tilde{T}_0(\vec{r})\equiv T_0+\eta(\vec{r})$, where $T_0=T_c+3\beta^2/(16\alpha_T\gamma)$ is the equilibrium transition temperature in the clean limit. As a consequence, local regions of the high-temperature phase may exist below T_c.

III. NUMERICAL RESULTS

In this section we present the numerical results obtained by solving the model introduced previously. A complete description requires the appropriate numerical values for the parameters, here taken from experimental data for Fe-Pd.[17] In reduced units: $\beta=-276\kappa/l_0^2$, $\gamma=4.86\times10^5\kappa/l_0^2$, $A_3=4.54\kappa/l_0^2$, and $A_1=2.27\kappa/l_0^2$. We set κ, T_c, and α_T equal to unity, leading to a length scale of $l_0=0.23925$ nm. Simulations have been carried out on a square lattice of linear size $L=10^3l_0$, discretized on a 512×512 mesh, subjected to periodic boundary conditions. In the present simulations, variations in the elastic anisotropy $\mathcal{A}$ have been implemented by changing the value of A_3. Simultaneously, we set the ratio[20] $A_3/A_1=2$. Starting from a randomly and slightly distorted configuration, the system evolves according to a purely relaxational dynamics toward a stabilized configuration.

Disorder is defined on the coarse-grained mesh, which introduces finite local differences of T_c, denoted by $\Delta T_c(\vec{r})$. As a consequence, a distribution of finite local free-energy barriers arises, separating regions of the system with differ-

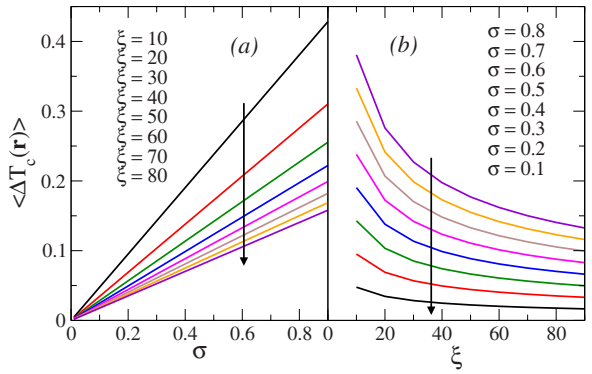

FIG. 1. (Color online) Mean finite local differences of T_c, denoted by $\langle \Delta T_c(\vec{r}) \rangle$, as a function of σ for different values of (a) ξ and (b) vice versa.

ent metastability regimes. As discussed below, if the long-range anisotropic interactions are not strong enough, the system is not able to overcome such barriers and may freeze in metastable, glassy states.

The dependence of the mean value of $\Delta T_c(\vec{r})$, denoted by $\langle \Delta T_c(\vec{r}) \rangle$, on both σ and ξ is shown in Figs. 1(a) and 1(b), respectively. Looking at the slope of the curves, it is easy to note that the dependence of $\langle \Delta T_c(\vec{r}) \rangle$ on ξ is strong only for relatively low values of ξ and high values of σ. With respect to this we have carried out simulations analogous to those presented here for a smaller value of ξ (ξ=10) in order to check the effect of variations in this parameter. We have found that they do not affect qualitatively either the results or the conclusions. Consequently, from now on, we keep $\xi = 20 l_0$ constant and focus our attention on the effect of σ. We shall return to this point again.

In Fig. 2 we show snapshots of selected structural patterns at $T=0.5<T_c$ (well inside the low-temperature regime) and for different values of A_3 and σ. In order to highlight the differences among the configurations, at their right side we have plotted the diffraction patterns, corresponding to the

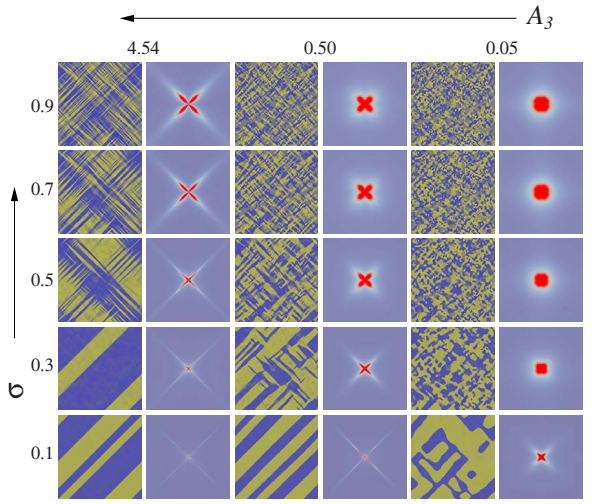

FIG. 2. (Color online) Illustrative phase diagram at low temperature (T=0.5) for different values of A_3 (~elastic anisotropy $\mathcal{A}$) and disorder intensity σ. Each configuration is shown with its corresponding Fourier-transformed intensity $|\mathbf{F}(e_2)|^2$.

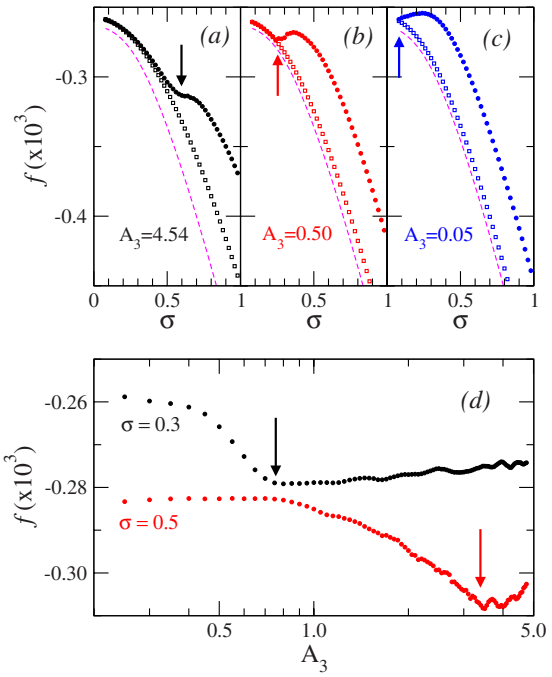

FIG. 3. (Color online) [(a)–(c)] Averaged free-energy density f as a function of σ for three different values of A_3. Filled symbols are obtained starting from the highest value σ=0.98 and gradually decreasing σ whereas empty symbols have been obtained by increasing σ starting from the lowest value σ=0.08. Arrows indicate the values of σ below which twin formation is allowed. Dashed lines indicate just the Landau free-energy contribution. (d) f as a function of A_3 for two different values of σ. Arrows point to the critical value of A_3 above which twins exist. For more details see the text.

intensity of the Fourier transform $|\mathbf{F}(e_2)|^2$, averaged over 20 independent realizations of disorder. Several overall trends can be identified in Fig. 2. (i) From left to right the texture loses directionality as reflected in the diffraction pattern that changes from a crosshatched to a circular shape. This is consistent with decreasing anisotropy. (ii) From bottom to top the domain size decreases, consistent with the increase in σ and the associated energy barriers. This is confirmed by the widening of the diffraction pattern toward higher values of the wave vector. (iii) Twin boundaries exist only for low values of σ. Actually, as we shall demonstrate later, they appear for the values of disorder below a critical σ^*, which in turn depends on A_3 in such a way that the higher A_3 the higher σ^*. (iv) Crosshatched patterns are obtained for high values of both A_3 and σ. We notice that, although such patterns are characteristic of tweed precursors, in the present case they correspond to low-temperature structures that, as discussed below, exhibit some glassy features. From now on we shall refer to it as *glassy tweed*. (v) Finally, for the lowest value A_3=0.05, ramified dropletlike structures are observed. In fact, only for very low values of σ the pattern shows some directionality.

In order to compare the relative stability of the relaxed structures, in Fig. 3 we show the behavior of the free-energy density f (averaged over 40–200 realizations of disorder) as a function of both σ and A_3. The upper panels show the

dependence of f on σ for the same three values of A_3 as in Fig. 2. Filled symbols have been obtained by gradually decreasing σ from the highest value $\sigma=0.98$, for which glassy states exist. Actually, we have checked that they are very close to those obtained independently (as those shown in Fig. 2), i.e., those that can be observed experimentally. On the contrary, empty symbols have been obtained by increasing σ gradually, starting from the lowest value $\sigma=0.08$. At this low value, twins are easily formed and, once created, they survive despite the increase in σ. Consistently, one can observe that f is always lower in the σ-increasing curve than in the σ-decreasing one. Actually, the former may be considered as the free energy of the global minimum and any deviation between the two curves provides a measure of the degree of metastability of the latter. In fact, the existence of such global minimum proves that the origin of the metastability is kinetic, as opposed to geometrically frustrated systems (like the paradigmatic antiferromagnetic triangle). Additional arguments explaining this kinetic origin are discussed in Sec. IV. Globally, in both curves, the total free energy decreases with increasing σ. This is because the Landau free-energy contribution (here represented by the dashed lines) prevails over the other terms (Ginzburg and long-range anisotropic terms) and becomes more and more negative as the number of regions with high $\tilde{T}_c(\vec{r})$ increases. Interestingly, focusing on the σ-decreasing curve, f exhibits an anomaly around a particular value of σ (denoted by an arrow) which depends on A_3. This is precisely the critical disorder $\sigma^*(A_3)$ above which long-range twins cease to exist. Indeed, the deviation of f from the free energy of the global minimum increases remarkably for $\sigma > \sigma^*$. This is a signature of the degree of metastability of the nontwinned states. For completeness, in Fig. 3(d) we have plotted the dependence of f on A_3 for two values of σ. Again, the behavior of f reveals the existence of an anomaly around a critical value A_3^* (denoted by an arrow) which depends on σ. Twins are only observed for $A_3 > A_3^*$. Similar to case (a), for $A_3 < A_3^*(\sigma)$ the system is no longer able to reach the twinned state, resulting in an increase in f and therefore in metastability. All these features are consistent with the configurations observed in Fig. 2.

So far, we have focused on the large metastability associated with untwinned low-temperature configurations. However, metastability is a necessary but not a sufficient condition to prove the existence of glassy states. Thus, in order to detect possible glassy behavior, we have carried out ZFC/FC simulation experiments. Figure 4 shows two cases of ZFC/FC results in order to illustrate the behavior of both ZFC and FC curves. The FC curve is a smooth, monotonically decreasing curve with increasing T, as expected. However, despite some qualitative differences between (a) (high A_3 and σ) and (b) (low A_3 and σ) in both cases the ZFC curve exhibits deviation from the FC curve below a certain *splitting* temperature. This is indicative of glassy behavior.

Figure 5 shows the ZFC curves obtained for different values of σ and A_3. Here the FC curves have been omitted for clarity and their behavior is in all cases very similar to those in Fig. 4. In the three cases (a)–(c) one observes that glassy behavior is obtained for values of σ above a critical value that exactly coincides with that obtained previously from the

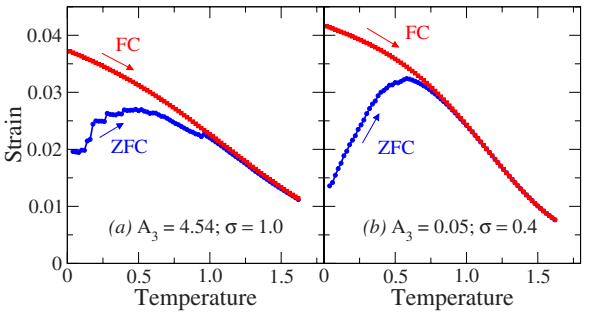

FIG. 4. (Color online) ZFC/FC curves for two different values of A_3 and σ.

behavior of f. We can then conclude that metastability observed in Fig. 3 does indicate glassy states. A comparison with Fig. 4 in Ref. 7 reveals that, indeed, similar effects are obtained either by reducing anisotropy or increasing disorder. Moreover, some small but important differences can still be observed between these cases, as can be seen for $A_3 = 4.54$, in case (a), with respect to other cases. Note that these differences may be better noticed in Fig. 4, between the (a) and (b) cases. The ZFC curve is more flat than for lower values of A_3 [cases (b) and (c)], indicating a more blocked dynamics that prevents the system from reaching the FC curve. The low stress field is not able to make the system

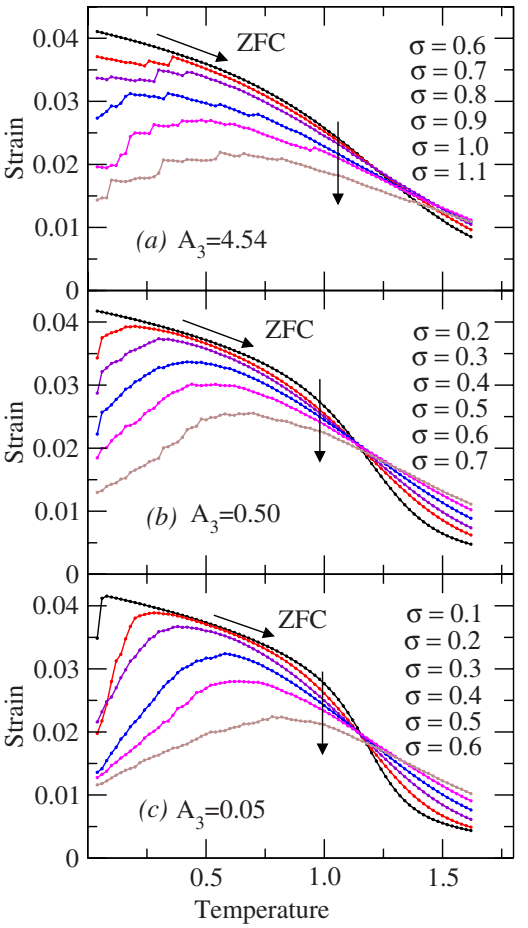

FIG. 5. (Color online) ZFC curves for different values of A_3 and σ. Vertical arrows indicate progressively increasing values of σ.

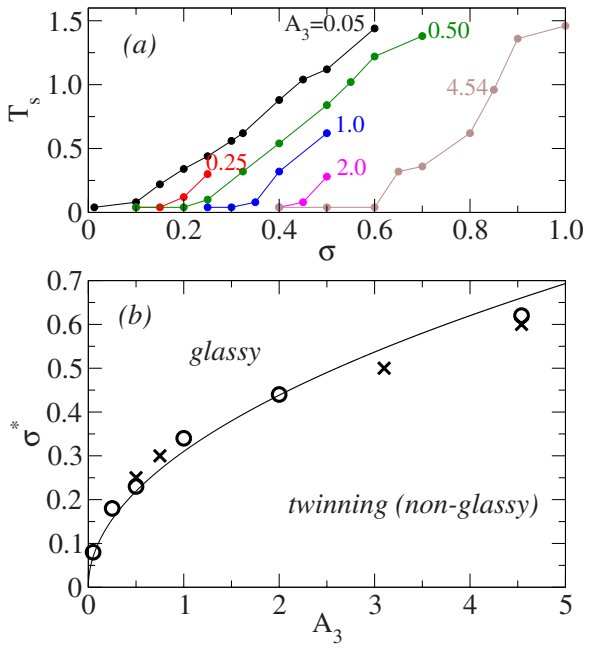

FIG. 6. (Color online) (a) Splitting temperature (T_s) as a function of disorder for different values of anisotropy. (b) Points indicate the crossover behavior in the material parameters. Glassy behavior is obtained for high values of disorder with respect to anisotropy and for low values of anisotropy with respect to disorder. Circles correspond to the vanishing T_s in (a) whereas crosses correspond to the arrows in Fig. 3. The continuous line is the function $\sigma^* \sim \sqrt{A_3}$.

evolve smoothly toward the monovariant state. Instead, some small, sharp jumps are observed due to the sudden correlations of different, broken domains of a particular variant (selected by the stress field) that start to become connected. After a certain number of jumps, the system does reach the monovariant state and thus the FC curve. In that sense, the same factor (i.e., the anisotropy) that for $\sigma < \sigma^*(A_3)$ enables the system to form long-range twinned structures, for $\sigma > \sigma^*(A_3)$, however, causes a higher degree of freezing than for lower values of A_3. Actually, this can be related to the behavior of f in Figs. 3(a)–3(c), where it can be observed that in the glassy regime $[\sigma > \sigma^*(A_3)]$, the degree of metastability (i.e., the larger the deviation from the free energy in the global minimum) increases with A_3 whereas in the twinned regime $[\sigma < \sigma^*(A_3)]$ all the curves approximately coincide.

Figure 6(a) shows the splitting temperatures T_s (i.e., the temperatures at which ZFC starts to deviate from FC curve) as a function of disorder and for different values of anisotropy. For martensite (twinned structures) T_s drops to zero whereas in the glassy regime T_s increases with σ. Also, for a given value of disorder, the higher the anisotropy the lower the T_s. Moreover, for low values of anisotropy, T_s shows a regular behavior (constant slope) whereas at high values of A_3, the T_s dependence becomes more irregular, consistent with the jumping behavior mentioned above. The disorder values at which T_s vanishes indicate that the ZFC deviation (glassy behavior) starts to arise. Figure 6(b) displays the crossover behavior in terms of critical values for the model

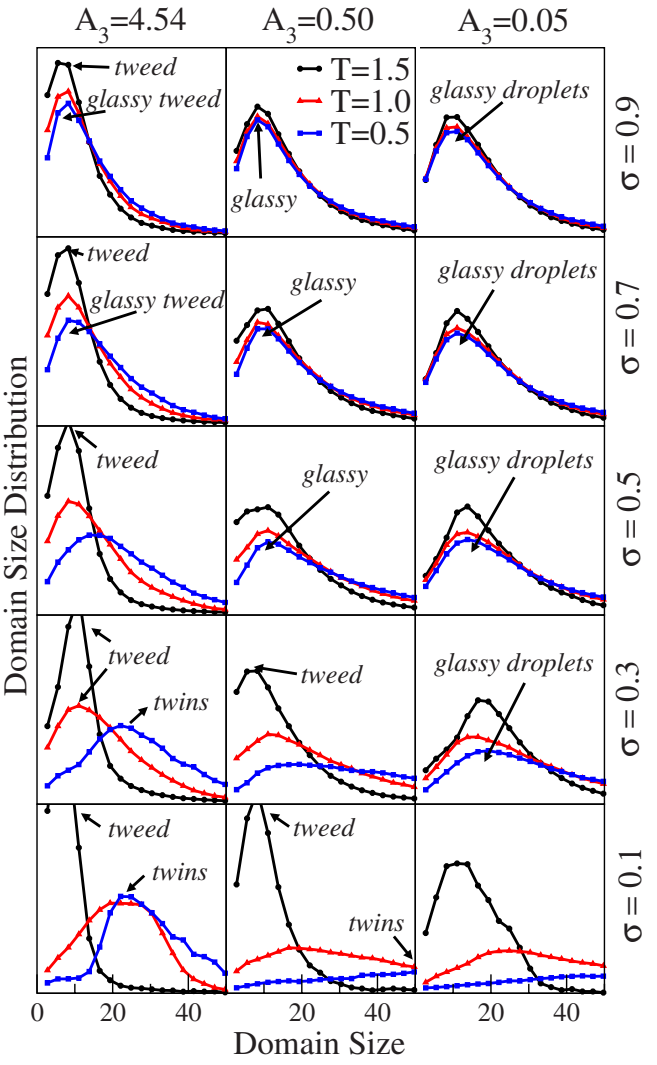

FIG. 7. (Color online) Domain size distribution for the same values of σ and A_3 as used in Fig. 2 and for three different temperatures: in the parent phase ($T=1.5$), near the transition temperature ($T=1.0$) and in the martensitic phase ($T=0.5$). The corresponding patterns are specified in the unambiguous cases. Glassy states are obtained in those cases where the characteristic domain sizes do not change by decreasing T, thus indicating freezing of the structures. Same vertical scale (in arbitrary units) applies to all cases.

parameters $\sigma^*(A_3)$. Circles are taken from the vanishing T_s in Fig. 6(a) whereas crosses are taken from the arrows in Fig. 3. We have found that such a crossover behaves approximately as $\sigma^* \sim \sqrt{A_3}$ (indicated by the curve).

Finally we have studied the effect of temperature in the different twinned/glassy regions by analyzing the domain size from the high- to the low-temperature regime. Figure 7 shows the domain size distribution for the same values of σ and A_3 as in Fig. 2 and for three different temperatures: $T=1.5$ ($>T_0>T_c$), $T=1.0$ ($=T_c$), and $T=0.5$ ($<T_c$). For relatively high anisotropy and small σ values—martensitic systems in the small figures at the bottom left corner—tweed precursor is found at high T with a characteristic length that changes toward the characteristic length of twins[21] when undergoing the MT. Instead, when σ is high enough to block twin formation, the characteristic domain size at high T sur-

vives when T is lowered well below the transition. Domains are not allowed to grow due to the presence of relatively high levels of disorder but freeze thus rendering the system to anchor in metastable, glassy states. Note that the values $\{\sigma, A_3\}$ for which domains freeze coincide with those that cause glassy behavior in the previous figures.

For completeness, let us state that variations in ξ in our model mainly affect the high-σ regime. Particularly, for a given A_3, a decrease in ξ results in a decrease in σ^* and conversely. Moreover, such decrease is greater for higher values of σ^*, consistent with the dependence of $\langle \Delta T_c(\vec{r}) \rangle$ on ξ, shown in Fig. 1. The results are not presented here for clarity since they do not contribute to any additional physical insights.

IV. DISCUSSION

In the present work we have systematically studied the dependence of textures and ZFC/FC behavior of martensitic systems on the elastic anisotropy as well as the intensity of disorder. The obtained ZFC/FC behavior indicates broken ergodicity in the glassy state in agreement with experimental results[11] in $Ni_{51.5}Ti_{48.5}$.

For this purpose, we first scanned the low-T configurational diagram as a function of both parameters σ and A_3. We observed that twinning only occurs for sufficiently high A_3 with respect to σ. In the $\{\sigma, A_3\}$ region in which twins are not observed, we have found that the observed textures exhibit glassy features by studying the ZFC/FC behavior. This is consistent with the analysis in the parameter region of the free energy f as well as the evolution of the mean domain size with change in temperature. In the glassy region f exhibits high degree of metastability that increases with increasing A_3. The domain size remains constant upon cooling for pairs of values $\{\sigma, A_3\}$ that exhibit glassy features whereas in the nonglassy region the domain size grows when decreasing the temperature. This indicates that the origin of the present glassy behavior is related to kinetic freezing rather than that arising from possible geometrical frustration.

In order to understand this glassy behavior, ZFC/FC simulations are of particular interest. It is clear that the effect of applying a stress field on the system leads to the selection of a variant, thus attempting to transform the other variant into the preferred one. In the case of martensitic twins, low stress fields succeed in this attempt and are able to transform the disfavored variant regions completely. In this context, long-range anisotropic elastic interactions provide the system with easy ways to carry out the transformation. This is reflected in the fact that ZFC and FC curves coincide. On the other hand, glassy states behave differently. Under the same low fields, the system is not able to transform completely all the regions due to the presence of disorder that breaks long-range correlations and blocks the transformation, being able to partially retain the system in a disordered state. Looking at the free energy, by increasing the temperature the energy barriers are lowered, making it easier for a given region to transform the variant. This is why in the ZFC curve the total strain increases with increasing temperature up to a certain value, where it exhibits a peak. Typically the peak in ZFC curve is close to the corresponding value in the FC curve, i.e., close to the splitting point. Then one can deduce that the system is no longer glassy and achieves the monovariant state, i.e., the global minimum of energy. Increasing the temperature implies decreasing the equilibrium value of strain and therefore the total strain, too. Upon heating above the transition temperature, given that the stress field is low enough, the system will transform into a slightly deformed austenite state and therefore the global strain will vanish almost completely. Upon cooling and heating again, the system will follow a monovariant state due to the presence of the stress field.

In principle one could expect the appearance of domains to be deliberate due to surviving long-range interactions, although weak or partially blocked by the presence of disorder. In that sense, long-range anisotropic interactions would not be able to induce a strong directionality in the domain structure due to disorder but would establish a particular short-range distribution of nondirectional domains by promoting the selection of a particular variant for each domain during its evolution. This selection could depend on the surrounding configuration of domain variants due to a possible tendency toward global strain minimization. Then, by decreasing the temperature, the corresponding growth of these domains would create a low-temperature configuration with a particular disordered domain distribution that would be geometrically frustrated[22] since the system would not be able to achieve the minimum of energy due to the thermodynamic reasons mentioned above.

However, simulations with strictly zero anisotropy and thus with no long-range effects also show glassy behavior. Since in the absence of long-range interactions the total free energy becomes local, no energetic reasons persist to promote the selection of a particular variant in different emerging domains, but it occurs independently from each other. This supports the idea that glassy behavior has a dynamical origin (kinetic freezing) and excludes the hypothesis of geometrical frustration. At that point we have checked that the correlations between emerging domains at high T are independent of the corresponding variant.

Long-range anisotropic potential has a power-law falloff. This means that no length scale is associated with such interactions but they affect the whole system in which they act. Nevertheless, the presence of disorder creates energy barriers that, for a range of certain critical values (that does depend on the anisotropy), are able to screen the long-range potential, breaking correlations, and the corresponding twin structures. For low values of anisotropy, the critical value of disorder is also low and the system becomes short ranged, and purely disorder driven, giving rise to a glassy ramified droplet structure, as observed experimentally.[11] However, for high values of anisotropy, the critical value of disorder is high and the system does not become short ranged as in the low-$\{\sigma, A_3\}$ case. Although the twins are broken as well, glassy tweed textures persist at low temperatures, as a successful compromise between the two factors. Here, the system is both anisotropy driven and disorder driven (whereas twinning is only anisotropy driven) and exhibits the typical length scales similar to the usual high-T tweed precursor. Experiments also demonstrate that systems with high $\mathcal{A}$ need high levels of disorder to inhibit twin formation.[23] The simu-

lations carried out in this paper show that glassy behavior is also expected in such systems and that the fine details of ZFC behavior should be different. In that sense, our simulations provide guidance on how to proceed experimentally, in particular, to verify the crossover behavior predicted in Fig. 6(b).

ACKNOWLEDGMENTS

This work was supported by CICyT (Spain) under Project No. MAT2007-61200, DURSI (Catalonia) under Project No. 2005SGR00969, and the U.S. Department of Energy. P.Ll. acknowledges support from DGICyT (Spain).

[1] Z. Nishyiama, *Martensitic Transformations* (Academic, London, 1978).
[2] S. Muto, R. Oshima, and F. Fujita, Acta Metall. Mater. **38**, 685 (1990).
[3] E. K. H. Salje, *Phase Transitions in Ferroelastic and Co-elastic Crystals* (Cambridge University Press, Cambridge, 1990).
[4] L. E. Tanner, A. R. Pelton, and R. Gronski, J. Phys. (Paris) **43**, 169 (1982).
[5] K. Otsuka and X. Ren, Prog. Mater. Sci. **50**, 511 (2005).
[6] Y. Murakami, H. Shibuya, and D. Shindo, J. Microsc. **203**, 22 (2001).
[7] P. Lloveras, T. Castán, M. Porta, A. Planes, and A. Saxena, Phys. Rev. Lett. **100**, 165707 (2008).
[8] Values near the transformation temperature.
[9] R. Oshima, M. Sugiyama, and F. E. Fujita, Metall. Trans. A **19**, 803 (1988).
[10] S. Sarkar, X. Ren, and K. Otsuka, Phys. Rev. Lett. **95**, 205702 (2005).
[11] Y. Wang, X. Ren, K. Otsuka, and A. Saxena, Phys. Rev. B **76**, 132201 (2007).
[12] Note that we are using the same notation as used in magnetism in order to emphasize the analogy between both problems. The characterization of the magnetic ZFC/FC experiments has been, for instance, studied in detail in S. Nagata, P. H. Keesom, and H. R. Harrison, Phys. Rev. B **19**, 1633 (1979).
[13] V. Cannella and J. A. Mydosh, Phys. Rev. B **6**, 4220 (1972).
[14] B. Martínez and X. Obradors, Ll. Balcells, A. Rouanet, and C. Monty, Phys. Rev. Lett. **80**, 181 (1998).
[15] D. Viehland, J. F. Li, S. J. Jang, L. E. Cross, and M. Wuttig, Phys. Rev. B **46**, 8013 (1992).
[16] A. M. Bratkovsky, S. C. Marais, V. Heine, and E. K. H. Salje, J. Phys.: Condens. Matter **6**, 3679 (1994).
[17] S. Kartha, J. A. Krumhansl, J. P. Sethna, and L. K. Wickham, Phys. Rev. B **52**, 803 (1995).
[18] S. R. Shenoy, T. Lookman, A. Saxena, and A. R. Bishop, Phys. Rev. B **60**, R12537 (1999).
[19] Note also that the harmonic coefficients are directly related to second-order elastic constants: $A_1=C_{11}+C_{12}$, $A_2=C_{11}-C_{12}=2C'$, and $A_3=4C_{44}$.
[20] We have checked that variations in this value do not affect the relevant results presented here.
[21] In fact, ZFC/FC simulations are carried out in a model with periodic boundary conditions. This gives rise to a global minimum consisting of a monovariant state. However, pure relaxational dynamics takes our system to twinned metastable states but with no characteristic length. In real martensites surface effects make the global minimum to consist of an equal-length twinning (i.e., with a characteristic length) in order to minimize the surface and the total energy. This is not expected to modify the relevant results concerning ZFC/FC simulations. However, in order to obtain this characteristic length of twins, some other simulations with no periodic boundary conditions but with austenitic boundary conditions have been carried out.
[22] R. Moessner and A. P. Ramirez, Phys. Today **59**(2), 24 (2006).
[23] X. Ren (private communication); see also, Y. Wang. X. Ren. K. Otsuka, and A. Saxena, Acta Mater. **56**, 2885 (2008).